Removal of arsenic by magnetic biochar prepared from pinewood and natural hematite

CrossMark

Shengsen Wang [a,b], Bin Gao [c,*], Andrew R. Zimmerman [d], Yuncong Li [a,b], Lena Ma [b], Willie G. Harris [b], Kati W. Migliaccio [a,c]

[a] Tropical Research and Education Center, University of Florida, Homestead, FL 33031, United States
[b] Soil and Water Science Department, University of Florida, Gainesville, FL 32611, United States
[c] Department of Agricultural and Biological Engineering, University of Florida, Gainesville, FL 32611, United States
[d] Department of Geological Sciences, University of Florida, Gainesville, FL 32611, United States

HIGHLIGHTS

- Magnetic biochar was prepared from pine wood and natural hematite.
- Hematite modified biochar showed greater ability to remove aqueous As.
- γ-Fe_2O_3 particles on the biochar served as sorption sites for As.

ARTICLE INFO

ABSTRACT

There is a need for the development of low-cost adsorbents to removal arsenic (As) from aqueous solutions. In this work, a magnetic biochar was synthesized by pyrolyzing a mixture of naturally-occurring hematite mineral and pinewood biomass. The resulting biochar composite was characterized with X-ray diffraction (XRD), X-ray photoelectron spectroscopy (XPS), scanning electron microscopy (SEM) and energy-dispersive X-ray analysis (EDS). In comparison to the unmodified biochar, the hematite modified biochar not only had stronger magnetic property but also showed much greater ability to remove As from aqueous solution, likely because the γ-Fe_2O_3 particles on the carbon surface served as sorption sites through electrostatic interactions. Because the magnetized biochar can be easily isolated and removed with external magnets, it can be used in various As contaminant removal applications.

© 2014 Elsevier Ltd. All rights reserved.

1. Introduction

Arsenic (As) is a carcinogenic trace metal that is toxic to human and animals. It occurs naturally in soils and can be mobilized by weathering reactions and biological activity and may lead to contamination of surface or groundwater aquifers (Mohan and Pittman, 2007). In addition, anthropogenic As contamination by discharge and disposal of As-containing compounds may lead to even greater As concentrations (Mandal and Suzuki, 2002). Because of the severe toxicity of As to humans, a very strict drinking water allowance limit of $10\ \mu g\ L^{-1}$ was prescribed by the US Environmental Protection Agency.

Various removal techniques such as precipitation, adsorption, membrane separation, ion exchange and permeable reactive barriers, have been developed to treat As contaminated water and soils (Tuutijarvi et al., 2009). Among them, adsorption is the one of the most commonly used method for the removal of As from aqueous solutions (Mohan and Pittman, 2007). Many low-cost sorbents such as carbonaceous materials, clay minerals and metal oxyhydroxides, have been successfully applied for As sorption (Goldberg, 2002; Zhou et al., 2014). Several studies have demonstrated that As tends to accumulate on the surface of metal oxyhydroxides and clay minerals containing Fe, Mn, Al, Cu, and Co (Ferguson and Gavis, 1972; Mandal and Suzuki, 2002). Strong sorption of As from aqueous solution by Fe, Al, and Mn oxides and naturally occurring clay minerals, such as kaolinite, montmorillonite, and illite, has been reported frequently in the literature (Gimenez et al., 2007; Goldberg, 2002).

Hematite is one of the most abundant natural iron oxide minerals and shows good As sorption ability (Gimenez et al., 2007). The sorption behaviors and mechanisms of As on hematite have been investigated for various solution chemistry conditions (Goldberg and Johnston, 2001). Using X-ray scattering analysis, Catalano

et al. (2008) found that the sorption of As on hematite was mainly controlled by electrostatic interactions to form inner and outer sphere surface complexes. Surface complex models have also successfully simulated experimental sorption data (Goldberg, 2002). Several studies have synthesized iron oxides to mimic the natural hematite and found that the synthesized hematite showed better As sorption ability because of higher purity and larger surface area (Auffan et al., 2008). In addition, thermal treatment has also been used to 'activate' hematite to enhance its sorption ability to As in aqueous solution (Ramirez-Muniz et al., 2012).

Biochar is a pyrogenic carbon material produced by combustion of biomass under oxygen limited conditions. Because of its unique properties such as high surface area and cation exchange capacity, biochar can be used for such applications as soil improvement, fertility enhancement and carbon sequestration (Mohana et al., 2014; Zimmerman et al., 2011). It also has shown great potential to remove heavy metals from aqueous solution and to reduce their mobility and bioavailability in soils (Ahmad et al., 2014; Zhou et al., 2013). Because the surfaces of most of the biochars are predominantly net negatively charged (Mukherjee et al., 2011; Yao et al., 2012), their sorption of aqueous As, which is in anionic forms of either arsenate (As(V)) or arsenite (As(III)), is relatively low (Beesley and Marmiroli, 2011). Several methods have thus been developed to modify biochar to enhance its sorption of As. In particular, biochar modified with colloidal and nano-sized oxyhydroxides showed strong ability to remove As from aqueous solution (Chen et al., 2011; Zhang and Gao, 2013). For example, iron oxide-biochar composites prepared by either pyrolyzing iron chloride (FeCl$_3$)-modified biomass or precipitating Fe^{3+}/Fe^{2+} on biochar surfaces greatly enhanced the As sorption ability of the biochars (Chen et al., 2011; Zhang et al., 2013). However, the methods used to create these biochar nanocomposites are relatively complex and costly. Thus, additional investigations thus are needed to develop simple and cost-effective methods to modify biochars with iron oxide particles, particularly with natural iron oxide minerals.

The objective of this work was to develop and evaluate a new method to prepare iron-oxide biochar composites from biomass and natural hematite. Hematite-treated pinewood was used as the feedstock to produce the biochar through pyrolysis. Physicochemical properties of the resulting biochar were measured in laboratory and sorption ability of the biochar to As was assessed through batch sorption experiments.

2. Methods

2.1. Reagents

All chemicals used in this work were analytical grade and were dissolved in deionized (DI) water (18.2 MΩ) (Nanopure water, Barnstead). Sodium arsenate dibasic heptahydrate (Na$_2$HAsO$_4$·7H$_2$O) was purchased from Fisher Scientific. A natural hematite mineral specimen was obtained from Wards Natural Science Establishment, Inc. (Minnesota, USA) and X-ray diffraction (XRD) analysis confirmed it to be nearly pure, with only trace amounts of kaolinite and quartz. The mineral was crushed with hammer and ground with a pestle and mortar and sieved to particle sizes of between 38 and 75 μm for use in subsequent experiments. Commercial loblolly pine (Pinus taeda) wood was oven dried overnight at 80 °C and then chopped with a mechanic mill. The crushed feedstock was then sieved to between 0.425 and 1 mm.

2.2. Biochar preparation

The method of preparing hematite modified biochar was similar to that used by Yao et al. (2014). A hematite suspension was prepared by mixing 2 g of crushed mineral particles in 40 mL of DI water. The suspension was stirred and sonicated for 30 min with an ultrasonicator (3510R-DTH, Bransonic Ultrasonics Corporation) to form a stable suspension. About 10 g of the feedstock was well mixed with the suspension for 2 h and was then oven-dried at 80 °C. The hematite-treated biomass was pyrolyzed in a tube furnace (MTI, Richmond, CA) under N$_2$ at a peak temperatures of 600 °C for one hour. Feedstock without modification procedure was used as control and went through the same pyrolysis process. The biochars produced were sieved to obtain particles between 0.075 and 0.425 mm and rinsed with DI water several times. Biochar was then oven dried overnight at 80 °C and saved in a sealed container for later use. The biochars with and without hematite modification were denoted as HPB and PB, respectively.

2.3. Characterizations

Total carbon (C), nitrogen (N), and hydrogen (H) content in the biochar samples were analyzed with a CHN Elemental analyzer (Carlo-Erba NA-1500). The inorganic element content of the biochar samples were determined using acid digestion method and analyzed by inductively coupled plasma-atomic emission spectrometry (ICP-AES, Perkin–Elmer Plasma 3200). Oxygen was determined as the weight difference between the raw dried biochar and sum of C, H, N, and other non-volatile elements.

Total surface area was measured using N$_2$ sorption on a NOVA 1200 analyzer and calculated using Brunauer–Emmett–Teller (BET) method. Scanning electron microscope (SEM) images were obtained with a JEOL JSM-6400 Scanning Microscope. Energy dispersive X-ray spectroscopy (EDS, Oxford Instruments Link ISIS) was coupled with SEM to examine surface elemental composition and obtain surface elemental distribution maps.

Surface elemental composition was also analyzed by X-ray photoelectron spectroscopy (XPS) with a PHI 5100 series ESCA spectrometer (Perkin–Elmer). An Al X-ray source was used with a 93.90 eV passing energy between 0 and 1400 eV binding energy. High-energy resolution scans of Fe2p and C1s peaks were obtained with pass energy of 23.50 eV in the 705–734 eV and 281–293 eV binding energy ranges, respectively.

Surface crystallinity was analyzed to identify Fe-bearing minerals using an X-ray diffractometer (XRD) (Philips Electronic Instruments) equipped with a stepping motor, a graphite crystal monochromator, and a CuKα radiation source.

Thermal stability of PB and HPB was examined using thermogravimetric analysis (TGA) with a Mettler Toledo's TGA/DSC1 analyzer. Temperature was increased by 10 °C per minute between 25 and 700 °C under air atmosphere.

2.4. Sorption kinetics and isotherm

Sorption kinetics of As at a constant concentration (20 mg L^{-1}) onto biochar were examined using the method of Zhang and Gao (2013). Briefly, about 0.05 g of biochar (2.5 g L^{-1}) was added to 20 mL As solutions (pH ~7) in 68 mL digestion vessels (Environmental Express) at room temperature (22 ± 0.5 °C). The vessels with sorption mixtures were placed on a shaker and agitated at 50 rpm until sampling. At each sampling time (0.5, 1, 2, 4, 8, 12, 24 and 48 h), the suspensions were immediately filtered through 0.22 μm pore size nylon membrane filters (GE cellulose nylon membrane). Concentrations of As in the filtrates were determined with an inductively coupled plasma-atomic emission spectrometry (ICP-AES, Perkin–Elmer Plasma 3200) and the residues were examined spectroscopically as described above. Sorbed As(V) was calculated as the difference in As concentration between initial and final solution. Kinetics data were fitted using various kinetic models (detailed in Supporting Information).

Adsorption isotherms were constructed using 20 mL solutions As(V) concentrations ranging 1–50 mg L^{-1} with biochar (2.5 g L^{-1}). The suspension was agitated on a shaker for 24 h, a period of time determine to be sufficient to have reached apparent sorption equilibrium, and then treated as described above. Isotherm data were simulated with various isotherm models (as described in Supporting Information).

3. Results and discussion

3.1. Biochar properties

Elemental analysis showed that the Fe content of the HPB was 118 times greater than that of the PB (Table 1) due to the addition of hematite. This is also supported by the higher ash content of HPB after combustion at 700 °C under air (Table 1). The amounts of volatile elements such as C, H, and N, and non-volatile elements such as Ca, K, and P in the HPB were lower, due to the dilution effects of the hematite addition. Because hematite also has Al and Mg, the modification also slightly increased their contents in the HPB (Table 1). The BET N$_2$ surface area decreased only slightly after hematite addition suggesting that (1) hematite had a specific surface area similar to that of the pristine biochar, and (2) the added hematite did not block pore openings of the biochar.

TGA analysis showed the HPB to be slightly more thermally stable than the pristine biochar, beginning to decompose at a higher temperature (Fig. 1) due to thermally inactive hematite serving as a diluent.

The SEM/EDS analyses of the HPB suggest that pyrolysis soldered and stabilized the hematite particles on carbon surfaces (Fig. S1, Supporting Information). SEM image (Fig. S1A and S1E) clearly show many small aggregates/particles stabilized on HPB surfaces, which were not found on the PB surfaces (Fig. S2, Supporting Information). The EDS mapping of carbon (Fig. S1B and S1F), oxygen (Fig. S1C and S1G), and iron (Fig. S1D and S1H) were used to identify the surface elemental compositions, where the dark particles in the carbon map (absence of C) matched well with the light areas on iron and oxygen (presence) maps. XPS analysis of the HPB showed that the binding energies of Fe2p1/2 and Fe2p3/2 were 710.85 and 724.48 eV, respectively (Fig. S3, Supporting Information). These values are close to reported values for Fe^{3+} (Zhang et al., 2013; Zhong et al., 2006), indicating that the iron particles on the biochar surface are Fe$_2$O$_3$.

Although the original hematite is weakly magnetic, the HPB demonstrated strong magnetic property and could be easily attracted by a permanent magnet (Fig. S4, Supporting Information). This result indicated that the pyrolysis process not only produced the hematite-biochar composites but also 'activated' the magnetic property of the hematite. Previous studies have shown that thermal treatment can enhance the magnetic properties of hematite (Mansilla et al., 2002; Zhang et al., 2012). Natural hematite is mainly made of α-Fe$_2$O$_3$ with rhombohedral structure, which has weak magnetic property, whereas thermally-treated hematite may have maghemite (γ-Fe$_2$O$_3$), cubic structures with strong magnetic properties (Zhang et al., 2012). Comparisons of the XRD patterns of the original hematite with that of the HPB sample suggests that the pyrolysis process did alter the crystal structure of the
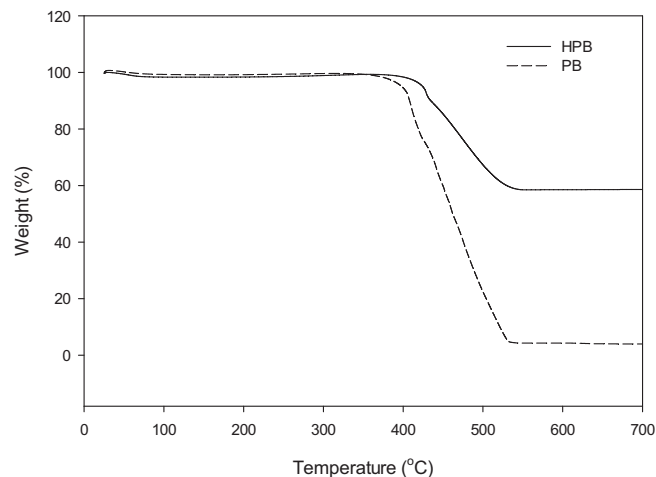

Fig. 1. Thermogravimetric analysis (TGA) of pine biochar (PB) and hematite modified biochar (HPB).

hematite of the HPB (Fig. S5, Supporting Information). The d-spacing of the original hematite used in this work matched well with the values from published database for natural hematite minerals (Schimanke and Martin, 2000). The diffraction pattern of the HPB (Fig. S5B), however, was different from the hematite but close to maghemite (γ-Fe$_2$O$_3$) (Fig. S5A). The Bragg peaks of XRD pattern of the HPB were at 30.2°, 35.5°, 43.2°, 57.3°, and 62.9°, which can be assigned to γ-Fe$_2$O$_3$ (Schimanke and Martin, 2000; Zhang et al., 2013).

3.2. Sorption kinetics

The sorption of As to both the PB and the HPB samples showed two phases: a rapid initial sorption during the first two hours followed by a much slower phase till reaching sorption equilibria after roughly 20 h (Fig. 2A). The first phase could be ascribed to rapid occupation of easily accessible external surface sorption sites such as outer sphere complexation (Essington, 2004). The slow phase could be related to the formation of inner layer complexes (Essington, 2004). Alternatively, the slower phase may be related to kinetic inhibition of As movement through narrow pore channels. In comparison with the PB, the HPB showed faster and higher sorption of As, suggesting that the γ-Fe$_2$O$_3$ particles may serve as adsorption sites for As in aqueous solution.

Several sorption kinetic models were applied to simulate the experimental data (Table S1, Supporting Information). Among all the tested models, Elovich model, an empirical model, described the As sorption kinetics the best (Table 2). This suggests that the sorption of As onto the biochar samples may be controlled by multiple interaction mechanisms or processes (Sparks, 1999).

3.3. Sorption isotherm

The sorption isotherms of As onto the two biochar samples were "L" shape (Fig. 2B), which is commonly observed for As

Table 1
Elemental composition and surface area of pinewood biochar (PB) and hematite-modified biochar (HPB).

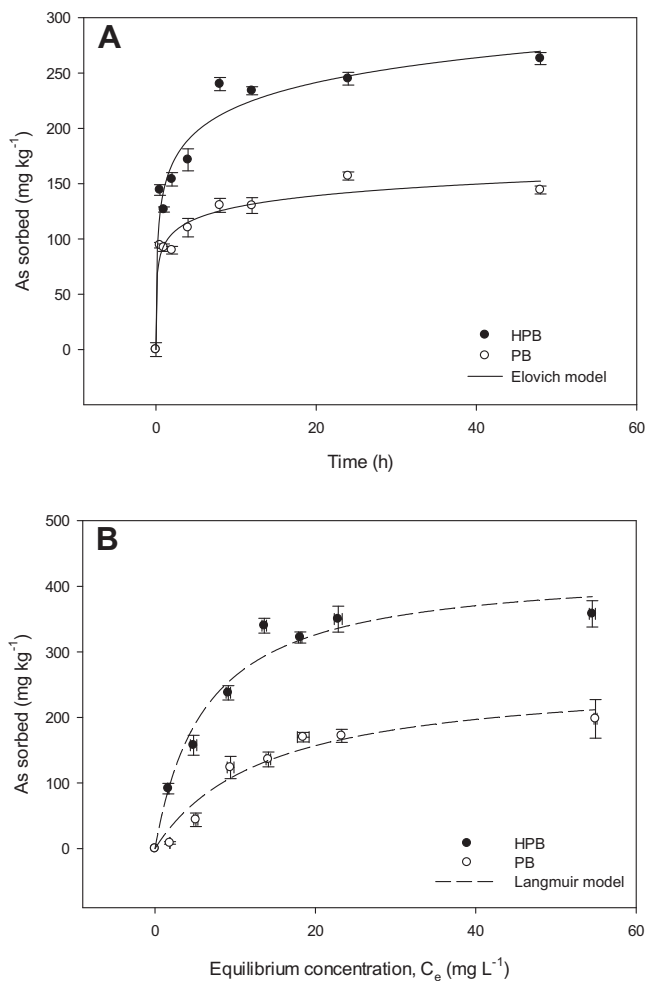|	C	N	H	O	Fe	Al	Ca	Mg	K	P	BET surface area m^2 g^{-1}
	%, mass										
PB	85.7	0.3	2.1	11.4	0.02	0.04	0.19	0.12	0.05	0.04	209.6
HPB	51.7	0.2	1.4	43.1	2.95	0.24	0.10	0.14	0.04	0.03	193.1

Fig. 2. Kinetics (A) and isotherm (B) data and fitted models for As(V) sorption by loblolly pinewood biochar (PB) and hematite-modified biochar (HPB). Error bars represent standard deviation.

Langmuir model is the most common model used to describe monolayer adsorption processes, it has also be used to describe the sorption of chemical compounds on composited materials (Yao et al., 2011; Zhang et al., 2013) including As onto iron oxide nanoparticles or onto iron oxide-biochar nanocomposites (Chowdhury et al., 2011; Zhang et al., 2013). Values of the Langmuir maximum sorption capacity of As for PB and HPB were 265 and 429 mg kg^{-1}, respectively, also indicating that the hematite modification roughly doubled the As sorption ability of the biochar. The Langmuir maximum sorption capacity of As of HPB is lower than that of an iron oxide-biochar nanocomposites developed by Zhang et al. (2013), but it is similar to that of sorption capacity of magnetic biochars derived from chemical treated agricultural residuals (Chen et al., 2011).

3.4. Sorption mechanisms

Because both PB and HPB removed As from aqueous solution, the sorption of As onto HPB could be controlled by multiple processes associated with both carbonaceous and iron oxide surfaces. Previous studies have suggested that biochar can encourage the formation of precipitates which can then remove anions and cations, such as lead and phosphate, from aqueous solutions (Inyang et al., 2012, 2011; Yao et al., 2013). The XRD analysis of the post-sorption biochar samples did not show any new peaks (Fig. S5C), suggesting that no new minerals formed and the precipitation mechanism may not be important for As removal by HBP.

The sorption of As onto a solid surface is most likely controlled by two factors, namely speciation of the As and the charge of the sorbent surface (Tuutijarvi et al., 2009). Under the tested experimental conditions (pH ~7), As(V) mainly exists as $HAsO_4^{2-}$. Some of the functional groups of the biochar are protonated and thus positively charged as the point of zero charge for biochar pyrolyzed at 600 °C is usually above 7 (Mukherjee et al., 2011). As a result, the $HAsO_4^{2-}$ may interact with the positively charged functional groups on both PB and HPB surfaces through electrostatic attractions. In addition, iron oxide also has a pH dependent charge derived from protonation and deprotonation of surface —OH groups. The pH_{zpc} of the iron oxide particles on the HPB surfaces is around 7.5 (Chowdhury et al., 2011; Tuutijarvi et al., 2009), therefore, they are also predominantly positively charged under the tested experimental conditions. As a result, both the iron particles and surface functional groups of the HPB can serve as the sorption site for As in aqueous solution, which explains why the hematite modification greatly enhanced biochar's sorption ability to As. Previous studies have suggested that As adsorbed on surface functional groups and iron particle surfaces can be remobilized by alkaline regeneration agents, such as NaH_2PO_4 (Tuutijarvi et al., 2012). Because HPB is a low-cost adsorbent prepared from biomass and natural mineral, it may not be cost-effective to use chemical agents to regenerate the spent adsorbent. Further investigations, such as life-cycle cost analysis, thus are still needed to promote the application of HPB in As treatment.

sorption onto many carbonaceous sorbents (Chang et al., 2010; Zhang et al., 2013). Sorption of As onto both biochars increased with aqueous As concentration but seem to plateau at concentrations above 30–40 mg L^{-1}. Sorption of As onto the hematite-modified biochar was roughly double that of the pristine biochar at all concentrations, further suggesting that the iron oxide particles serve as adsorption sites with higher capacity for As in aqueous solution than the unmodified biochar.

Both Langmuir and Freundlich models were applied to simulate the sorption isotherms (Table S1). Although the two models both describe the experimental data well, the simulations of the Langmuir model fit the isotherms better (Table 2). Although

Table 2
Kinetics and isotherm models and best-fit parameters for As(V) sorption onto pinewood biochar (PB) and hematite modified biochar (HPB).

Model/equations	Biochar	Parameter 1	Parameter 2	R^2
		Kinetics		
Elovich	PB	α = 7856.2 mg kg^{-1}	β = 0.0665 mg kg^{-1}	0.961
$q_t = \beta^{-1}\ln(\beta\alpha t + 1)$	HPB	α = 2828.3 mg kg^{-1}	β = 0.0309 mg kg^{-1}	0.960
		Isotherm		
Langmuir	PB	S_{max} = 265.2 mg kg^{-1}	K = 0.0724 L mg^{-1}	0.951
$S = S_{max}KC/(1 + KC)$	HPB	S_{max} = 428.7 mg kg^{-1}	K = 0.159 L mg^{-1}	0.968

4. Conclusions

A magnetic biochar was synthesized by direct pyrolysis of hematite-treated biomass. The thermal treatment not only produced a biochar-based composite material, but also turned hematite into γ-Fe$_2$O$_3$ particles with strong magnetic properties. The γ-Fe$_2$O$_3$ particles can serve as sorption sites for As in aqueous solutions, and thus greatly improved the As removal ability of the biochar. Because both biomass and hematite mineral are low-cost natural materials that are abundant and inexpensive, the magnetic biochar developed in this work can be used as an alternative remediation agent in many environmental applications to mitigate the risks of As contamination.

Acknowledgement

Appendix A. Supplementary data

Supplementary data associated with this article can be found, in the online version, at http://dx.doi.org/10.1016/j.biortech.2014.10.104.

References

Ahmad, M., Rajapaksha, A.U., Lim, J.E., Zhang, M., Bolan, N., Mohan, D., Vithanage, M., Lee, S.S., Ok, Y.S., 2014. Biochar as a sorbent for contaminant management in soil and water: a review. Chemosphere 99, 19–33.

Auffan, M., Rose, J., Proux, O., Borschneck, D., Masion, A., Chaurand, P., Hazemann, J.L., Chaneac, C., Jolivet, J.P., Wiesner, M.R., Van Geen, A., Bottero, J.Y., 2008. Enhanced adsorption of arsenic onto maghemites nanoparticles: As(III) as a probe of the surface structure and heterogeneity. Langmuir 24 (7), 3215–3222.

Beesley, L., Marmiroli, M., 2011. The immobilisation and retention of soluble arsenic, cadmium and zinc by biochar. Environ. Pollut. 159 (2), 474–480.

Catalano, J.G., Park, C., Fenter, P., Zhang, Z., 2008. Simultaneous inner- and outer-sphere arsenate adsorption on corundum and hematite. Geochim. Cosmochim. Acta 72 (8), 1986–2004.

Chang, Q.G., Lin, W., Ying, W.C., 2010. Preparation of iron-impregnated granular activated carbon for arsenic removal from drinking water. J. Hazard. Mater. 184 (1–3), 515–522.

Chen, B.L., Chen, Z.M., Lv, S.F., 2011. A novel magnetic biochar efficiently sorbs organic pollutants and phosphate. Bioresour. Technol. 102 (2), 716–723.

Chowdhury, S.R., Yanful, E.K., Pratt, A.R., 2011. Arsenic removal from aqueous solutions by mixed magnetite–maghemite nanoparticles. Environ. Earth Sci. 64 (2), 411–423.

Essington, M., 2004. Soil and Water Chemistry – An Integrative Approach. CRC Press.

Ferguson, J.F., Gavis, J., 1972. A review of the arsenic cycle in natural waters. Water Res. 6 (11), 1259–1274.

Gimenez, J., Martinez, M., de Pablo, J., Rovira, M., Duro, L., 2007. Arsenic sorption onto natural hematite, magnetite, and goethite. J. Hazard. Mater. 141 (3), 575–580.

Goldberg, S., 2002. Competitive adsorption of arsenate and arsenite on oxides and clay minerals. Soil Sci. Soc. Am. J. 66 (2), 413–421.

Goldberg, S., Johnston, C.T., 2001. Mechanisms of arsenic adsorption on amorphous oxides evaluated using macroscopic measurements, vibrational spectroscopy, and surface complexation modeling. J. Coll. Interf. Sci. 234 (1), 204–216.

Inyang, M., Gao, B., Yao, Y., Xue, Y., Zimmerman, A.R., Pullammanappallil, P., Cao, X., 2012. Removal of heavy metals from aqueous solution by biochars derived from anaerobically digested biomass. Bioresour. Technol. 110, 50–56.

Inyang, M.D., Gao, B., Ding, W.C., Pullammanappallil, P., Zimmerman, A.R., Cao, X.D., 2011. Enhanced lead sorption by biochar derived from anaerobically digested sugarcane bagasse. Sep. Sci. Technol. 46 (12), 1950–1956.

Mandal, B.K., Suzuki, K.T., 2002. Arsenic round the world: a review. Talanta 58 (1), 201–235.

Mansilla, M.V., Zysler, R., Fiorani, D., Suber, L., 2002. Annealing effects on magnetic properties of acicular hematite nanoparticles. Phys. B Condens. Matter 320 (1–4), 206–209.

Mohan, D., Pittman Jr., C.U., 2007. Arsenic removal from water/wastewater using adsorbents—a critical review. J. Hazard. Mater. 142 (1–2), 1–53.

Mohana, D., Sarswata, A., Okb, Y.S., Jr., C.U.P., 2014. Organic and inorganic contaminants removal from water with biochar, a renewable, low cost and sustainable adsorbent – a critical review. Bioresour. Technol. 160, 191–202.

Mukherjee, A., Zimmerman, A.R., Harris, W., 2011. Surface chemistry variations among a series of laboratory-produced biochars. Geoderma 163 (3–4), 247–255.

Ramirez-Muniz, K., Jia, F., Song, S., 2012. Adsorption of As-V in aqueous solutions on porous hematite prepared by thermal modification of a siderite–goethite concentrate. Environ. Chem. 9 (6), 512–520.

Schimanke, G., Martin, M., 2000. In situ XRD study of the phase transition of nanocrystalline maghemite (γ-Fe$_2$O$_3$) to hematite (α-Fe$_2$O$_3$). Solid State Ion. 136–137, 1235–1240.

Sparks, D.L., 1999. Kinetics and mechanisms of chemical reactions at the soil mineral/water surface. In: Soil Physical Chemistry, Second ed. CRC Press LLC, pp. 135–191.

Tuutijarvi, T., Lu, J., Sillanpaa, M., Chen, G., 2009. As(V) adsorption on maghemite nanoparticles. J. Hazard. Mater. 166 (2–3), 1415–1420.

Tuutijarvi, T., Vahala, R., Sillanpaa, M., Chen, G., 2012. Maghemite nanoparticles for As(V) removal: desorption characteristics and adsorbent recovery. Environ. Technol. 33 (16), 1927–1936.

Yao, Y., Gao, B., Chen, J.J., Zhang, M., Inyang, M., Li, Y.C., Alva, A., Yang, L.Y., 2013. Engineered carbon (biochar) prepared by direct pyrolysis of Mg-accumulated tomato tissues: characterization and phosphate removal potential. Bioresour. Technol. 138, 8–13.

Yao, Y., Gao, B., Fang, J., Zhang, M., Chen, H., Zhou, Y., Creamer, A., Sun, Y., Yang, L., 2014. Characterization and environmental applications of clay-biochar composites. Chem. Eng. J. 242, 136–143.

Yao, Y., Gao, B., Inyang, M., Zimmerman, A.R., Cao, X.D., Pullammanappallil, P., Yang, L.Y., 2011. Removal of phosphate from aqueous solution by biochar derived from anaerobically digested sugar beet tailings. J. Hazard. Mater. 190 (1–3), 501–507.

Yao, Y., Gao, B., Zhang, M., Inyang, M., Zimmerman, A.R., 2012. Effect of biochar amendment on sorption and leaching of nitrate, ammonium, and phosphate in a sandy soil. Chemosphere 89 (11), 1467–1471.

Zhang, C.X., Paterson, G.A., Liu, Q.S., 2012. A new mechanism for the magnetic enhancement of hematite during heating: the role of clay minerals. Stud. Geophys. Geod. 56 (3), 845–860.

Zhang, M., Gao, B., 2013. Removal of arsenic, methylene blue, and phosphate by biochar/AlOOH nanocomposite. Chem. Eng. J. 226, 286–292.

Zhang, M., Gao, B., Varnoosfaderani, S., Hebard, A., Yao, Y., Inyang, M., 2013. Preparation and characterization of a novel magnetic biochar for arsenic removal. Bioresour. Technol. 130, 457–462.

Zhong, L.S., Hu, J.S., Liang, H.P., Cao, A.M., Song, W.G., Wan, L.J., 2006. Self-assembled 3D flowerlike iron oxide nanostructures and their application in water treatment. Adv. Mater. 18 (18), 2426–2431.

Zhou, Y., Gao, B., Zimmerman, A.R., Chen, H., Zhang, M., Cao, X.D., 2014. Biochar-supported zerovalent iron for removal of various contaminants from aqueous solutions. Bioresour. Technol. 152, 538–542.

Zhou, Y.M., Gao, B., Zimmerman, A.R., Fang, J., Sun, Y.N., Cao, X.D., 2013. Sorption of heavy metals on chitosan-modified biochars and its biological effects. Chem. Eng. J. 231, 512–518.

Zimmerman, A.R., Gao, B., Ahn, M.Y., 2011. Positive and negative carbon mineralization priming effects among a variety of biochar-amended soils. Soil Biol. Biochem. 43 (6), 1169–1179.